*Supporting Information*

# Exploration of Novel Xanthine Oxidase Inhibitors Based on 1,6-Dihydropyrimidine-5-Carboxylic Acids by an Integrated in Silico Study

Na Zhai [1], Chenchen Wang [1], Fengshou Wu [1], Liwei Xiong [1,2,*], Xiaogang Luo [1,3], Xiulian Ju [1], Genyan Liu [1,*]

[a] *Hubei Key Laboratory of Novel Reactor and Green Chemical Technology, School of Chemical Engineering and Pharmacy, Wuhan Institute of Technology, Wuhan 430205, China*

[b] *Hubei Key Laboratory of Plasma Chemistry and Advanced Materials, Wuhan Institute of Technology, Wuhan 430205, China*

[c] *School of Materials Science and Engineering, Zhengzhou University, No.100 Science Avenue, Zhengzhou 450001, China*

[*] *Correspondence: zhily2000@126.com (L.X.); liugenyan@yahoo.com (G.L.)*

**Table S1.** Chemical structures of the used non-purine XOIs with their actual $pIC_{50}$ values and docking scores.

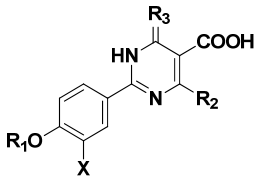


**Compounds 01-26: X = 1H-tetrazol-1-yl**
**Compounds 27-46: X = CN**

| No. | $R_1$ | $R_2$ | $R_3$ | $IC_{50}$ (μM) | $pIC_{50}$ | Docking score |
|---|---|---|---|---|---|---|
| 01 | methyl | H | O | 0.0920 | 7.0362 | 8.98 |
| 02 | *iso*-propyl | H | O | 0.0737 | 7.1325 | 8.94 |
| 03 | *iso*-butyl | H | O | 0.0644 | 7.1911 | 9.44 |
| 04 | *iso*-pentyl | H | O | 0.0541 | 7.2668 | 9.38 |
| 05 | allyl | H | O | 0.0437 | 7.3595 | 9.55 |
| 06 | *iso*-butenyl | H | O | 0.0569 | 7.2449 | 9.46 |
| 07 | *iso*-pentenyl | H | O | 0.0692 | 7.1599 | 9.21 |
| 08 | propinyl | H | O | 0.0500 | 7.301 | 9.47 |
| 09 | methylene cyclopropane | H | O | 0.0461 | 7.3363 | 9.73 |
| 10 | cyclopentyl | H | O | 0.0585 | 7.2328 | 9.51 |
| 11 | methylene cyclohexane | H | O | 0.0683 | 7.1656 | 9.46 |
| 12 | benzyl | H | O | 0.0945 | 7.0246 | 8.97 |
| 13 | *p*-methylbenzyl | H | O | 0.0894 | 7.0487 | 9.38 |
| 14 | *p*-tert-butylbenzyl | H | O | 0.1490 | 6.8268 | 9.12 |
| 15 | *p*-methoxylbenzyl | H | O | 0.0507 | 7.295 | 9.61 |
| 16 | *p*-fluorobenzyl | H | O | 0.0531 | 7.2749 | 9.53 |
| 17 | *p*-chlorobenzyl | H | O | 0.0691 | 7.1605 | 9.35 |
| 18 | *p*-bromobenzyl | H | O | 0.0552 | 7.2581 | 9.46 |
| 19 | *m*-methoxylbenzyl | H | O | 0.0516 | 7.2874 | 9.46 |
| 20 | *m*-fluorobenzyl | H | O | 0.0477 | 7.3215 | 9.76 |
| 21 | *m*-chlorobenzyl | H | O | 0.0288 | 7.5406 | 10.63 |
| 22 | *m*-bromobenzyl | H | O | 0.0450 | 7.3468 | 9.67 |
| 23 | *o*-chlorobenzyl | H | O | 0.0917 | 7.0376 | 9.10 |
| 24 | 2,5-dichlorobenzyl | H | O | 0.0639 | 7.1945 | 9.34 |
| 25 | 2,4-dichlorobenzyl | H | O | 0.0838 | 7.0768 | 9.37 |
| 26 | hydrogen | H | O | 0.6290 | 6.2013 | 7.85 |
| 27 | *iso*-propyl | H | O | 0.0916 | 7.0381 | 9.02 |
| 28 | *iso*-butyl | H | O | 0.0609 | 7.2154 | 9.55 |
| 29 | *iso*-pentyl | H | O | 0.0250 | 7.6021 | 10.51 |
| 30 | allyl | H | O | 0.0811 | 7.091 | 9.22 |
| 31 | *iso*-butenyl | H | O | 0.0336 | 7.4737 | 9.91 |
| 32 | *iso*-pentenyl | H | O | 0.0388 | 7.4112 | 9.68 |
| 33 | benzyl | H | O | 0.0387 | 7.4123 | 9.78 |
| 34 | *p*-fluorobenzyl | H | O | 0.0382 | 7.4179 | 9.75 |
| 35 | *p*-chlorobenzyl | H | O | 0.0499 | 7.3019 | 9.58 |
| 36 | *p*-bromobenzyl | H | O | 0.0298 | 7.5258 | 10.51 |
| 37 | *p*-tert-butylbenzyl | H | O | 0.1970 | 6.7055 | 8.35 |
| 38 | *p*-methylbenzyl | H | O | 0.0354 | 7.451 | 9.99 |

| | | | | | | |
|---|---|---|---|---|---|---|
| 39 | *iso*-pentyl | $CH_3$ | O | 0.5400 | 6.2676 | 8.40 |
| 40 | *iso*-butenyl | $CH_3$ | O | 0.5677 | 6.2459 | 8.36 |
| 41 | *p*-bromobenzyl | $CH_3$ | O | 0.1854 | 6.7319 | 9.01 |
| 42 | *p*-methylbenzyl | $CH_3$ | O | 0.1590 | 6.7986 | 8.81 |
| 43 | *iso*-pentyl | H | NH | 0.0240 | 7.6198 | 10.68 |
| 44 | *iso*-butenyl | H | NH | 0.0181 | 7.7423 | 10.69 |
| 45 | *p*-bromobenzyl | H | NH | 0.0271 | 7.567 | 10.50 |
| 46 | *p*-methylbenzyl | H | NH | 0.0339 | 7.4698 | 9.97 |

**Table S2.** The statistical results of other pharmacophore models using different compounds.

| No. | SPECIFICITY | N_HITS | FEATS | PARETO | ENERGY | STERICS | HBOND | MOL_QRY |
|---|---|---|---|---|---|---|---|---|
| 1 | 4.811 | 11 | 8 | 0 | 10.95 | 2156.90 | 562.20 | 95.77 |
| 2 | 4.803 | 12 | 8 | 0 | 11.80 | 2163.20 | 558.40 | 162.16 |
| 3 | 4.812 | 12 | 8 | 0 | 10.66 | 2143.50 | 562.30 | 87.70 |
| 4 | 5.638 | 11 | 8 | 0 | 10.54 | 2065.30 | 558.50 | 80.09 |
| 5 | 4.829 | 10 | 8 | 0 | 10.12 | 2191.80 | 561.10 | 95.43 |
| 6 | 4.808 | 12 | 8 | 0 | 8.20 | 2003.90 | 526.50 | 84.06 |
| 7 | 4.825 | 10 | 8 | 0 | 9.57 | 1847.80 | 548.20 | 76.72 |
| 8 | 4.824 | 11 | 8 | 0 | 11.54 | 2059.70 | 571.10 | 155.18 |
| 9 | 4.821 | 12 | 8 | 0 | 10.69 | 2267.10 | 584.60 | 78.31 |
| 10 | 4.822 | 11 | 8 | 0 | 24.33 | 2357.60 | 588.20 | 80.63 |

**Table S3.** The ADME prediction results of the non-ideal virtual-screened hits.

| Hit compound | MW (g/mol) | Fraction $Csp^3$ | Rotatable bonds | TPSA ($Å^2$) | GI absorption | BBB permeant | CYP1A2 inhibitor | CYP2C19 inhibitor | CYP2C9 inhibitor | CYP2D6 inhibitor | CYP3A4 inhibitor | Lipinski violations | SA score |
|---|---|---|---|---|---|---|---|---|---|---|---|---|---|
| VS01 (ZINC09434063) | 422.61 | 0.6 | 13 | 142.1 | Low | No | No | Yes | Yes | Yes | Yes | 0 | 3.43 |
| VS02 (ZINC04705438) | 421.52 | 0.27 | 7 | 111 | High | No | No | Yes | Yes | No | Yes | 0 | 3.97 |
| VS03 (ZINC59016051) | 429.47 | 0.2 | 9 | 126.8 | Low | No | No | Yes | Yes | No | Yes | 0 | 3.62 |
| VS04 (ZINC63625083) | 427.5 | 0.23 | 6 | 103.1 | High | No | No | No | No | No | No | 0 | 4.41 |
| VS05 (ZINC89942644) | 318.37 | 0.38 | 7 | 103.2 | High | No | No | No | No | No | No | 0 | 3.26 |
| VS06 (ZINC89942901) | 370.43 | 0.44 | 8 | 149 | Low | No | No | No | No | No | No | 0 | 4.02 |
| VS07 (ZINC04927833) | 411.52 | 0.27 | 11 | 101.5 | High | No | Yes | Yes | Yes | Yes | Yes | 0 | 3.51 |
| VS08 (ZINC95498920) | 347.43 | 0.63 | 6 | 50.8 | High | Yes | No | No | No | No | No | 0 | 3.75 |
| VS09 (ZINC39932293) | 412.49 | 0.58 | 10 | 176.7 | Low | No | No | No | No | No | Yes | 1 | 4.7 |
| VS10 (ZINC12537662) | 469.45 | 0.05 | 9 | 151.1 | Low | No | No | Yes | No | No | No | 1 | 3.6 |
| VS11 (ZINC12741060) | 480.51 | 0.38 | 11 | 123.9 | High | No | No | No | Yes | Yes | No | 0 | 4.95 |
| VS13 (ZINC24928355) | 295.34 | 0.33 | 7 | 127.2 | High | No | Yes | No | No | No | Yes | 0 | 2.76 |
| VS14 (ZINC06053573) | 389.36 | 0.28 | 9 | 139.6 | High | No | Yes | No | Yes | No | No | 0 | 4.22 |
| VS15 (ZINC31176221) | 402.45 | 0.32 | 5 | 96.8 | High | No | No | Yes | Yes | No | Yes | 0 | 3.72 |
| VS17 (ZINC21991916) | 332.33 | 0.75 | 12 | 151.6 | Low | No | No | No | No | No | No | 0 | 3.61 |
| VS18 (ZINC09493835) | 463.51 | 0.47 | 10 | 191.3 | Low | No | No | Yes | No | No | Yes | 0 | 3.73 |
| VS20 (ZINC65506066) | 308.33 | 0.11 | 5 | 57.9 | High | Yes | No | No | No | Yes | No | 0 | 2.6 |
| VS21 (ZINC09235475) | 426.4 | 0.09 | 5 | 120.3 | High | No | No | Yes | No | No | No | 0 | 3.46 |
| VS22 (ZINC32785893) | 582.65 | 0.27 | 12 | 123.9 | High | No | No | No | No | No | No | 0 | 5.15 |
| VS23 (ZINC21580816) | 418.4 | 0.09 | 8 | 122.1 | High | No | Yes | Yes | Yes | Yes | Yes | 0 | 2.97 |
| VS24 (ZINC63505952) | 498.61 | 0.33 | 8 | 71.5 | High | No | No | No | No | Yes | Yes | 0 | 5.42 |
| VS25 (ZINC09295542) | 453.81 | 0.1 | 7 | 133.8 | Low | No | No | Yes | No | No | No | 0 | 3.47 |
| VS27 (ZINC12820565) | 384.44 | 0.19 | 6 | 120.4 | High | No | Yes | Yes | Yes | Yes | Yes | 0 | 3.17 |
| VS28 (ZINC16362213) | 348.42 | 0.35 | 9 | 106.6 | High | No | Yes | Yes | Yes | No | Yes | 0 | 2.87 |
| VS29 (ZINC09120119) | 455.55 | 0.27 | 8 | 158.5 | Low | No | Yes | Yes | Yes | No | Yes | 0 | 4.11 |
| VS30 (ZINC72320942) | 432.56 | 0.42 | 8 | 79.9 | High | No | No | Yes | Yes | Yes | Yes | 0 | 4.42 |

| | | | | | | | | | | | | | |
|---|---|---|---|---|---|---|---|---|---|---|---|---|---|
| VS31 (ZINC12547951) | 387.48 | 0.26 | 9 | 111.1 | High | No | Yes | Yes | Yes | No | Yes | 0 | 3.46 |
| VS32 (ZINC39289590) | 248.3 | 0.5 | 3 | 38.3 | High | Yes | No | No | No | No | No | 0 | 2.68 |
| VS33 (ZINC73707897) | 398.48 | 0.41 | 10 | 71.6 | High | No | No | No | No | No | Yes | 0 | 4.03 |
| VS34 (ZINC18190685) | 481.52 | 0.3 | 12 | 186.9 | Low | No | No | No | No | No | Yes | 0 | 3.84 |
| VS35 (ZINC89942526) | 369.44 | 0.37 | 9 | 128.2 | High | No | No | No | No | No | No | 0 | 3.54 |
| VS36 (ZINC89943165) | 370.47 | 0.5 | 8 | 101.4 | High | No | No | No | No | No | No | 0 | 3.77 |
| VS37 (ZINC31167456) | 502.92 | 0.43 | 11 | 173.7 | Low | No | No | No | No | No | No | 1 | 5.28 |

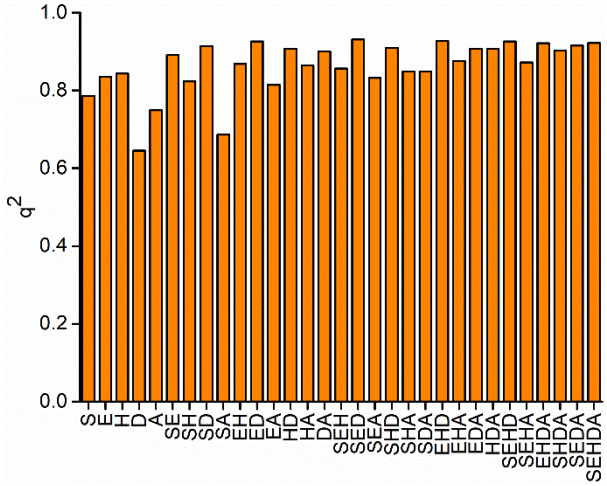


**Figure S1.** The $q^2$ values of all possible CoMSIA models with different field combinations (S: steric fields; E: electrostatic fields; H: hydrophobic fields; D: hydrogen-bond donor fields; A: hydrogen-bond acceptor fields).

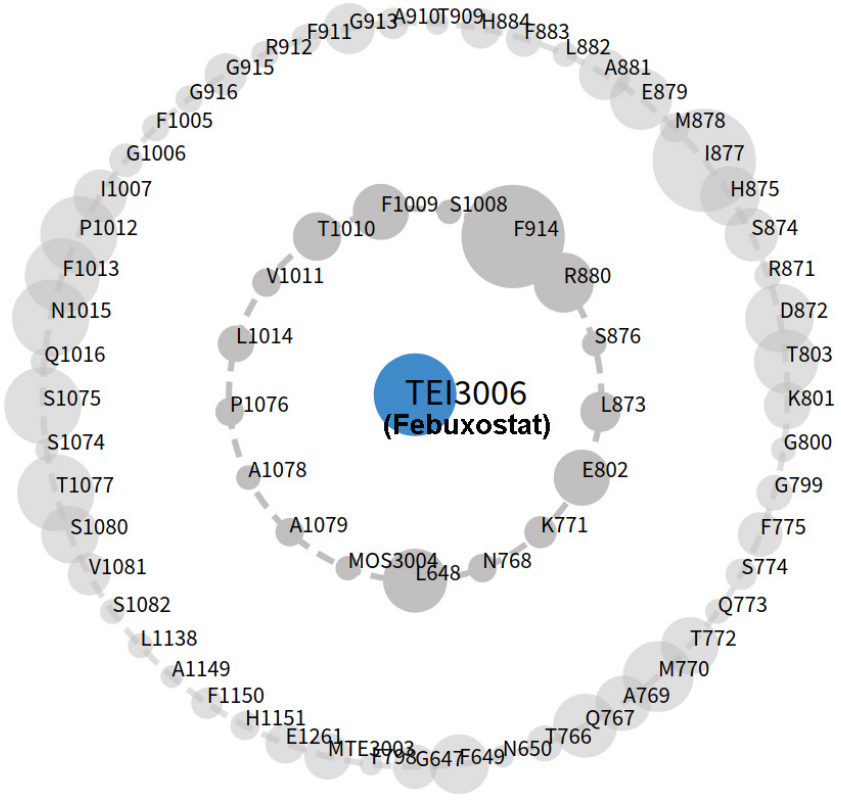


**Figure S2.** The asteroid plot of co-crystal XO structure (PDB ID: 1N5X) with febuxostat (center bule node).

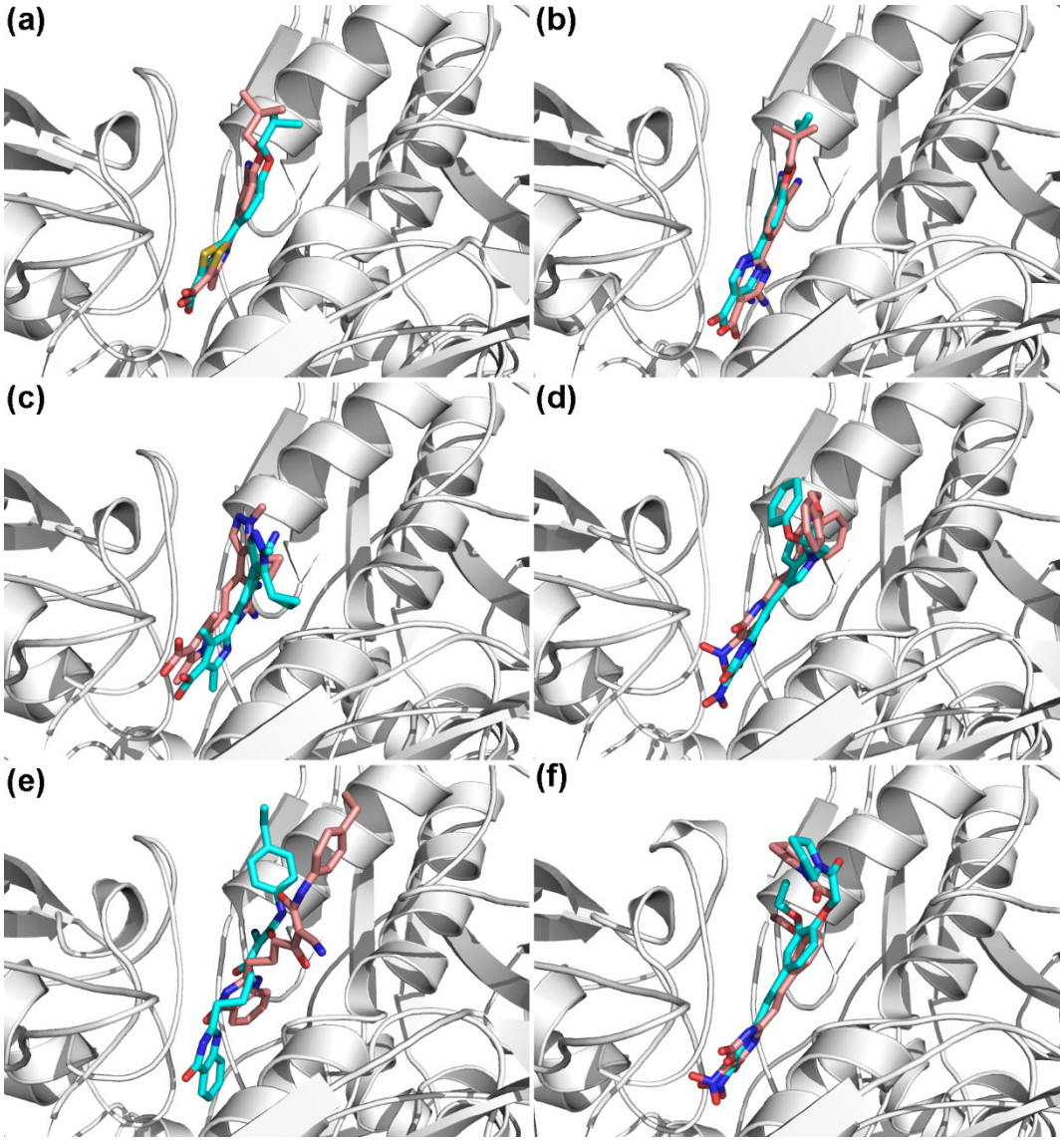


**Figure S3.** The initial (cyan sticks) and final (pink sticks) conformations of compounds febuxostat (a), **44** (b), **VS12** (c), **VS16** (d), **VS19** (e), and **VS26** (f) in XO protein during 50 ns MD simulations.

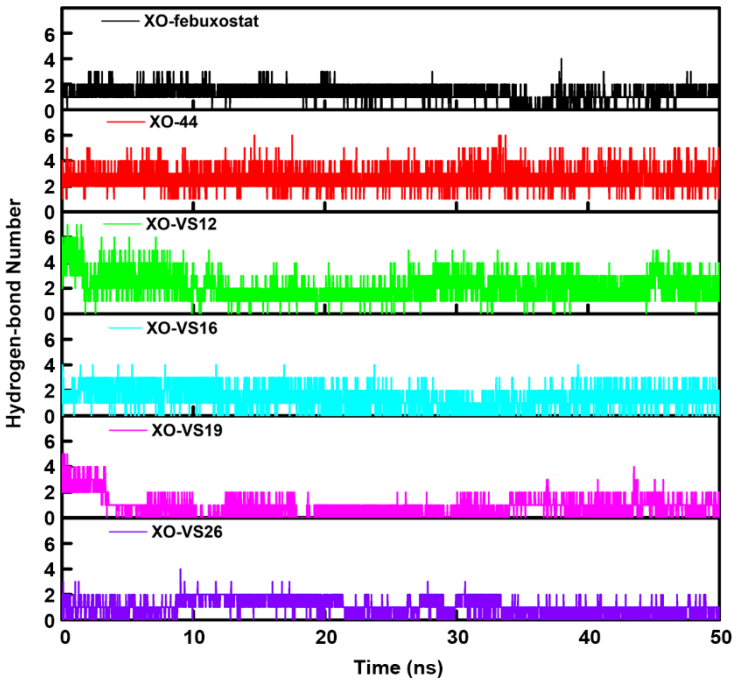


**Figure S4.** The hydrogen-bond numbers between protein and compounds febuxostat (black), **44** (red), **VS12** (green), **VS16** (cyan), **VS19** (magenta), and **VS26** (violet) during 50 ns MD simulations.

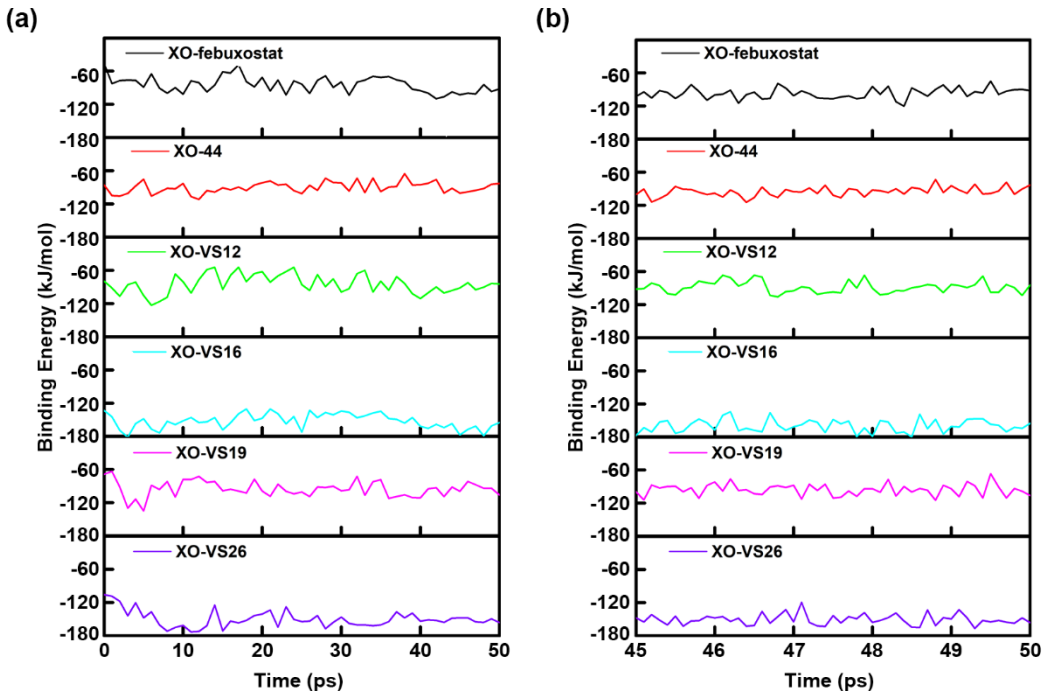


**Figure S5.** Binding energies (kJ/mol) convergence of complexes XO-febuxostat (black), XO-**44** (red), XO-**VS12** (green), XO-**VS16** (cyan), XO-**VS19** (magenta), and XO-**VS26** (violet) during 50 ns MD simulations (a: the 50 ns trajectory of each complex at an interval of 1 ns; b: the final 5 ns trajectory of each complex at an interval of 100 ps).


XO_bovine
XO_HUMAN

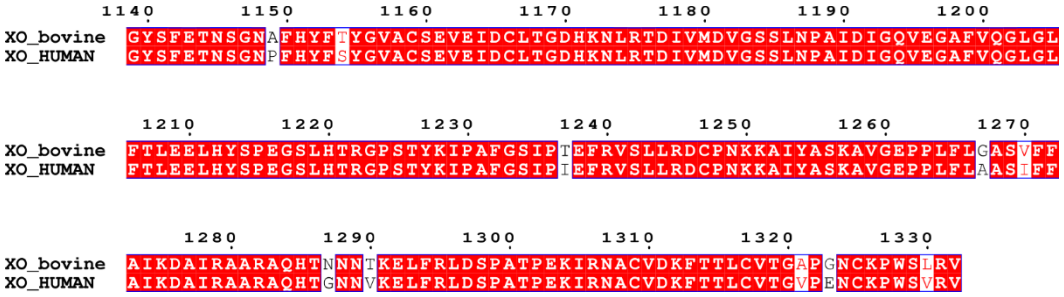


**Figure S6.** The sequence alignment of bovine and human XO enzymes (the key residues for febuxostat binding with XO marked by black frames).

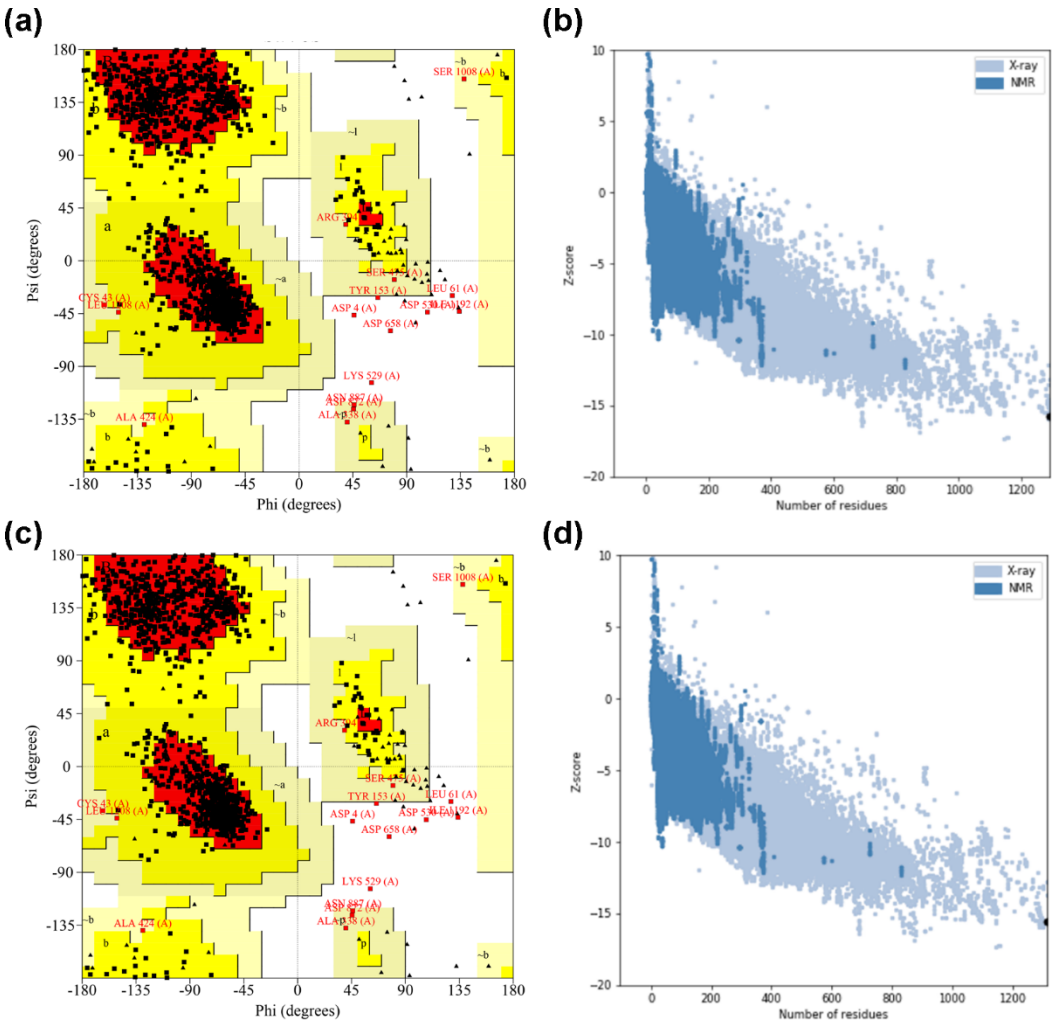


**Figure S7.** Evaluation results of Ramachandran (a, c) and Z-score distribution (b, d) plots of the original (a, b) and repaired (c, d) XO proteins.